Biochemical and Biophysical Research Communications 434 (2013) 541–546

Contents lists available at SciVerse ScienceDirect

Biochemical and Biophysical Research Communications

journal homepage: www.elsevier.com/locate/ybbrc

Metastasis suppressor Nm23-H1 inhibits STAT3 signaling via a negative feedback mechanism ☆

Lei Gong [a,1], Zhihao Wu [a,1], Lili Guo [a], Lin Li [a], Rongzhi Zhao [a,b], Daxing Zhu [a], Qinghua Zhou [a,*]

[a] Tianjin Key Laboratory of Lung Cancer Metastasis and Tumor Microenvironment, Tianjin Lung Cancer Institute, Tianjin Medical University General Hospital, Anshan Road No. 154, Heping District, Tianjin 300052, China
[b] Department of Radiation Oncology, Tianjin Medical University General Hospital, Anshan Road No. 154, Heping District, Tianjin 300052, China

ARTICLE INFO

Article history:
Received 1 March 2013
Available online 10 April 2013

Keywords:
Metastasis suppressor
STAT3 signaling
Negative feedback
Cancer metastasis
Transcriptional target

ABSTRACT

Persistent STAT3 activation is a critical event in tumorigenesis and metastatic progression. Recent studies have found higher levels of STAT3 in metastatic tissues than in primary tumor tissues. We speculated that such increased STAT3 activity might be attributed to a loss of function or reduction in expression of metastasis inhibitory protein during cancer progression, and we therefore examined the role of tumor metastasis-suppressor nm23-H1 in the activation of STAT3 in the A549 lung cancer cell line. We found that IL-6-dependent induction of tyrosine phosphorylation and activation of STAT3 were influenced by nm23-H1 inhibition. IL-6-induced $STAT3^{Tyr705}$ phosphorylation was significantly enhanced in A549 cells transfected with siRNA specific for nm23-H1, and the effect of nm23-H1 depletion on IL-6-induced $STAT3^{Tyr705}$ phosphorylation was reversed by ectopic expression of shRNA-resistant nm23-H1 protein. Moreover, STAT3 directly bound to the STAT3 binding site on the nm23-H1 promoter and activated its expression. Thus, we have identified a new feedback mechanism that might provide insight into an in-built metastasis-suppression function in tumor cells and which could be a logical new target for treatment of early metastatic disease.

1. Introduction

Lung cancer remains the leading cause of cancer-related deaths worldwide. The 5-year survival for lung cancer remains remarkably low owing to relapses and metastasis. A better understand is therefore needed of the molecular events that contribute to the invasion and metastasis of this disease. Signal transducer and activator of transcription 3 (STAT3) protein is constitutively activated in a wide variety of human cancers, and a functional contribution of activated STAT3 in lung carcinogenesis has been demonstrated in a number of recent studies [1–3]. Activated STAT3 not only upregulates genes that control cell proliferation, survival, and angiogenesis but also promotes metastasis. Importantly, recent studies showed higher levels of STAT3 expression in metastatic tissues than in primary tissues [4,5], suggesting a pivotal role of STAT3 in this process. We speculated that the increased STAT3 activity in metastasis might be attributed to a loss of function or reduction in expression of tumor metastasis inhibitory protein (metastasis suppressor) during cancer progression.

nm23-H1 was the first metastasis suppressor to be discovered, by Steeg et al. [6] in a mouse tumor model. Since then, nm23-H1 expression levels have been widely studied in many human tumor samples. An observed general pattern has been found that reduction or loss of nm23-H1 expression correlates with tumor progression and metastasis [7]. A similar pattern was validated by transfection of the nm23-H1 gene into several highly metastatic human tumor cell lines [8,9] and the nm23-H1 knockout mouse [10]. Despite extensive study, however, the mechanism by which nm23-H1 suppresses metastasis remains to be elucidated. We therefore examined the role of the tumor metastasis suppressor nm23-H1 in the activation of STAT3 in a lung cancer cell line.

2. Materials and methods

2.1. Cell culture and transfection

Cells of the human lung adenocarcinoma cell line A549 were maintained in RPMI 1640 medium supplemented with 10% fetal bovine serum. $A549^{shnm23\text{-}H1}$ cells with stably expressing nm23-H1-specific short hairpin RNA (shRNA) were obtained and

☆ Supported by grants from National Natural Science Foundation of China (No. 30973384), National Natural Science Foundation of China (No. 81272359), the Key Project from National Natural Science Foundation of China (No. 30430300), National 863 Program (No. 2006AAOZA401), National 973 Program (No. 2010CB529405), and the 211 Project Innovation Foundation of Tianjin Medical University for PhD Graduates (No. 2009GSI16).

* Corresponding author.
E-mail address: zhouqh1016@yahoo.com.cn (Q. Zhou).

[1] These authors contributed equally.

0006-291X/$ - see front matter © 2013 Elsevier Inc. All rights reserved.
http://dx.doi.org/10.1016/j.bbrc.2013.03.110

characterized in our laboratory by transducing A549 cells with a lentiviral construct containing the nm23-H1 shRNA sequence [11]. For transfection, cells were grown in six-well plates and transfected *in vitro* with PolyJet™ DNA transfection reagent (SignaGen Laboratories, Gaithersburg, MD) according to the manufacturer's protocol.

2.2. Cloning and DNA construction

nm23-H1 Promoter reporter constructs were generated by PCR amplification using purified genomic DNA as the template and the primers listed in Table 1. The PCR products were inserted into the Bgl II/Hind III sites of pGL3 basic vector (Promega, Madison, WI). nm23-H1 cDNA was generated by PCR amplification using purified total RNA as the template and the primers listed in Table 1. The PCR products were digested with BamHI/XbaI and inserted into the pcDNA3.1(+) vector. The plasmids STAT3, D/n-STAT3, and STAT3 reporter were provided by Gao (Department of Urology and Cancer Center, University of California at Davis, Sacramento, CA).

2.3. Small interfering RNA

The nm23-H1-specific small interfering RNA (siRNA) (sense: 5′-GGAACACUACGUUGACCUGtt-3′; anti-sense: 5′-CAGGUCAACGUA GUUCCtt-3′) was used to knockdown the expression of nm23-H1. Scrambled siRNA was used for control experiments. All the siRNA were purchased from Guangzhou RiboBio Company (Guangzhou, PR China). Cells were transfected with 10 nM of specific or control using 1 μL of GenMute™ siRNA and DNA transfection reagent (SignaGen Laboratories, Gaithersburg, MD). Cells were treated with interleukin-6 (IL-6) (Roche, San Francisco, CA) 24 h later.

2.4. Western blot analysis

Western blot analysis was performed as previously described [12] using specific antibodies against nm23-H1 (Santa Cruz, CA), $pSTAT3^{Tyr705}$, $pSTAT3^{Ser727}$, STAT3 (Cell Signaling Technology, Danvers, MA), and β-actin (Sigma–Aldrich, St. Louis, MO).

2.5. Quantitative real-time RT-PCR analysis

Total cellular RNA was isolated from cells using the Trizol reagent (Invitrogen, Camarillo, CA) according to the manufacturer's instructions and quantified using a UV spectrophotometer (Beckman Coulter, Los Angeles, CA). RNA (2 μg) was reverse transcribed using the M-MLV Reverse Transcriptase Kit (Promega) according to the manufacturer's protocol. The resultant cDNA (20 ng) was mixed with ABI SYBR Green Master Mix (Applied Biosystems, Carlsbad, CA) and primers for genes of interest and then amplified using the ABI7500 Real-time PCR System (Applied Biosystems) according to the manufacturer's protocol. The forward and reverse primers for each mRNA are shown in Table 1. The mean expression of the housekeeping gene GAPDH (glyceraldehyde-3-phosphate dehydrogenase) was used as an internal control. Each sample was analyzed in triplicate for each gene.

2.6. Dual luciferase reporter assays

A549 cells were plated onto 12-well plates, and transfections were performed at 60%–70% confluence. The nm23-H1 promoter reporter constructs in combination with Renilla luciferase control vector (pRL-CMV) were transfected along with relevant gene-specific expression plasmids. At 48 h post-transfection, the cell lysates were prepared, and firefly luciferase and Renilla luciferase were assayed according to the manufacturer's protocol (Promega). The firefly luciferase activity was normalized to that of Renilla luciferase. Each experiment was repeated three times in triplicate using a multimode microplate reader (TriStar LB941, Berthold Technologies, Germany).

2.7. Chromatin immunoprecipitation (ChIP) assay

ChIP assays were performed as previously described [12]. The resulting precipitated DNA samples were analyzed by PCR to amplify a 176-bp fragment of the nm23-H1 promoter with the following primers: forward, 5′-GCGAACGAAGGAAGTGAGTC-3′; reverse, 5′-AGAGCCCATTTTGCAGAACA-3′.

2.8. Site-specific mutagenesis

Point mutations in the nm23-H1 promoters 927Mut1 and 927Mut2 were generated by site-specific mutagenesis using the overlap PCR extension method. nm23-H1 promoter 927 was used as the template, and 927Mut1 PCR products were generated using primers A, 5′-AAAAAGATCTCCATTTTTGTACCTTTCCCCCGT-3′ (forward) and 5′-CGCTCACACGTTGCGTACCGTCCAAAGAGTGT-3′ (reverse); and primers B, 5′-GCACTCTTTGGACGGTACGCAACGTG TGAGCG-3′ (forward) and 5′-AAAAAAGCTTCACTTGCACGCACG-GAACG-3′ (reverse). 927Mut2 PCR products were generated using primers C, 5′-AAAAAGATCTCCATTTTTGTACCTTTCCCCCGT-3′ (forward) and 5′-AGAGCCCATTTTGCATCCCACCGCTCGCCCAC-3′ (reverse); and primers D, 5′-GTGGGCGAGCGGTGGGATGCAAAATGG GCTCT-3′ (forward) and 5′-AAAAAAGCTTCACTTGCACGCACG-GAACG-3′ (reverse). The PCR products were digested with Bgl II/Hind III and subcloned into the pGL3-luciferase vector. shRNA-resistant nm23-H1 cDNA was generated by PCR amplification using purified nm23-H1 cDNA-pcDNA3.1 plasmid as the template and the following primers: 5′-CGCGGATCCATGGCCAACTGTGAGCGAACATT-TATCGCCATCAAACCA-3′ (forward), 5′-GCTCTAGATCATTCATA-GATCCAGTTCTGA-3′ (reverse). Then PCR products were digested with BamHI/XbaI and subcloned into the pcDNA3.1(+) vector.

Table 1
Primers used for PCR amplifications.

Gene	Region	Primers
nm23-H1	−927 to +33	5′-AAAAAGATCTTAGATTGGTCTTTTGGTGTCGTC-3′ 5′-AAAAAAGCTTCACTTGCACGCACGGAACG-3′
nm23-H1	−705 to +33	5′-AAAAAGATCTCCATTTTTGTACCTTTCCCCCGTT-3′ 5′-AAAAAAGCTTCACTTGCACGCACGGAACG-3′
nm23-H1	−231 to +33	5′-AAAAAGATCTTCAGGCACTCTTTGGACTTCACG-3′ 5′-AAAAAAGCTTCACTTGCACGCACGGAACG-3′
nm23-H1	−149 to +33	5′-AAAAAGATCTAGAGAACCCGGGGGTGGAGAGAA-3′ 5′-AAAAAAGCTTCACTTGCACGCACGGAACG-3′
nm23-H1	+228 to +686	5′-CGCGGATCCATGGCCAACTGTGAGCGTACCT-3′ 5′-GCTCTAGATCATTCATAGATCCAGTTCTGA-3′
nm23-H1	+442 to +563	5′-AAAGGATTCCGCCTTGTTGGT-3′ 5′-GCCCTGAGTGCATGTATTTCAC-3′

2.9. Avidin–biotin complex DNA assay

A total of 1000 μg of untreated or IL-6-treated A549 whole-cell extract was incubated with 2 μg of biotinylated double-stranded oligonucleotides for 4 h with constant rotation at 4 °C in a total volume of 400 μl of immunoprecipitation buffer (50 mmol/L HEPES, 150 mmol/L NaCl, 1 mmol/L EDTA, 0.5% NP-40, 10% glycerol, 1 mmol/L dithiothreitol, 1 mmol/L phenylmethysulfonyl fluoride, and 5 mmol/L NaF). After the addition of 50 KL equilibrated streptavidin agarose beads (Sigma), incubation was continued

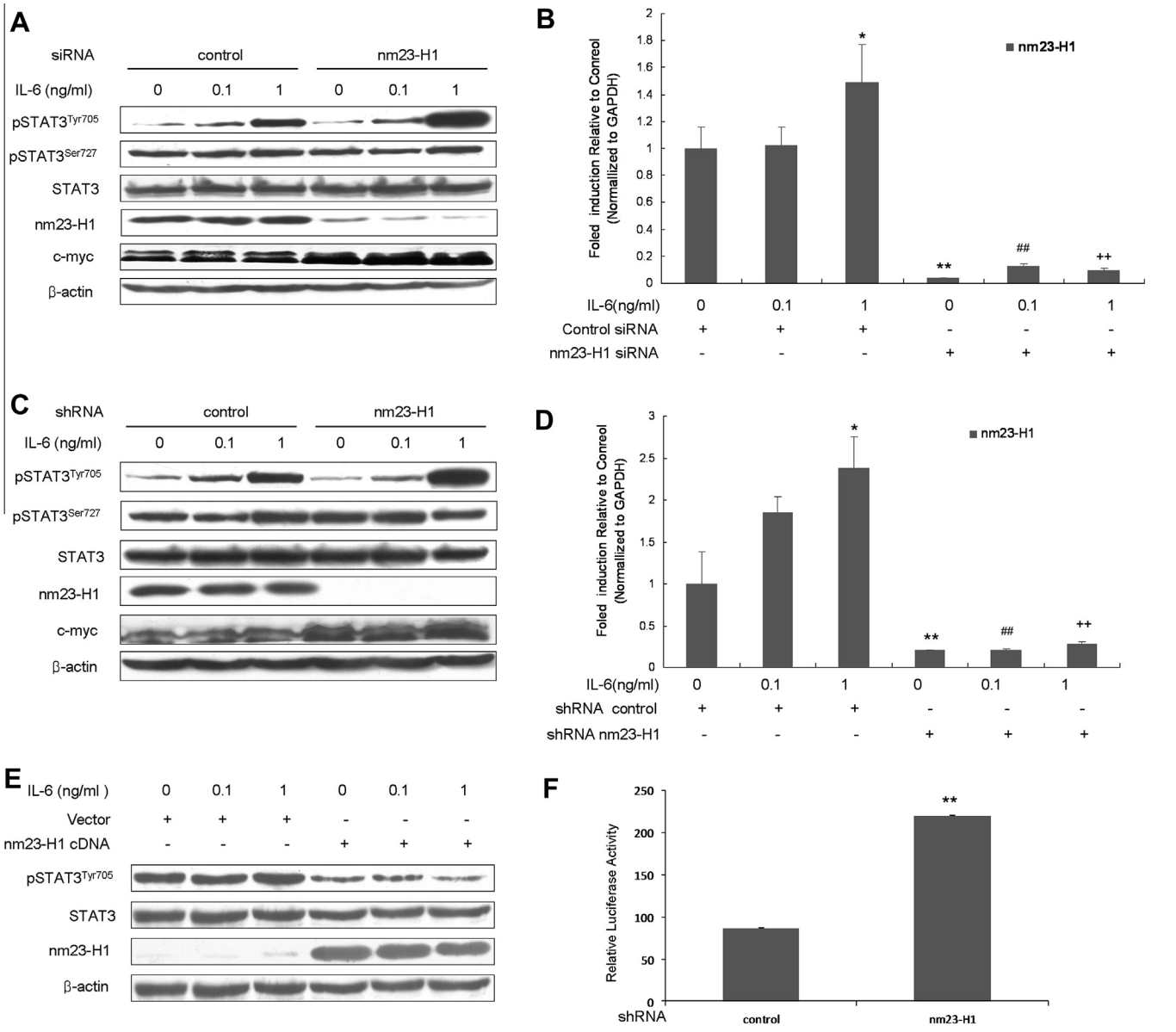

Fig. 1. nm23-H1 negatively regulates STAT3 activity. (A) A549 cells were seeded onto six-well plates and transfected with a control or nm23-H1-specific siRNA. At 48 h post-transfection, cells were left untreated or were treated with indicated amounts of IL-6 for an additional hour. Western blots were used to detect pSTAT3^{Tyr705}, pSTAT3^{Ser727}, total STAT3, nm23-H1, and c-Myc. Equal loading was demonstrated by probing with β-actin. Compared with control siRNA-treated cells, cells deficient in nm23-H1 showed significantly higher levels of IL-6-induced pSTAT3^{Tyr705}, the downstream target of c-Myc. (B) A549 cells transfected with a control or nm23-H1-specific siRNA were treated as described above in (A). Quantitative real-time PCR was performed for the analysis of mRNA expression levels of nm23-H1. Results are expressed as fold induction relative to cells without IL-6 treatment after normalization to the *GAPDH* expression. The graph showed efficient knockdown of nm23-H1 mRNA expression in cells transfected with an nm23-H1-specific siRNA and IL-6-induced fold induction of nm23-H1 mRNA levels of A549 cells transfected with a control siRNA ($^{*}p < 0.05$ and $^{**}p < 0.01$ for the difference from the cells transfected with control siRNA without treatment; $^{\#\#}p < 0.01$ for the difference from the 0.1 ng/mL IL-6-treated cells transfected with control siRNA; $^{++}p < 0.01$ for the difference from the 1 ng/ml IL-6-treated cells transfected with control siRNA by ANOVA for multiple comparison). (C). A549 cells were stably transfected with a control and an nm23-H1-specific shRNA expression vector and treated with the indicated amounts of IL-6 for 1 h or were left as untreated control in serum-free medium. Western blot analysis of pSTAT3^{Tyr705}, pSTAT3^{Ser727}, total STAT3, nm23-H1, c-Myc, and control β-actin showed that IL-6-induced STAT3 phosphorylation was significantly enhanced in nm23-H1-depleted cells. (D) Expression levels of nm23-H1 mRNA were monitored by quantitative real-time PCR in A549 cells stably transfected with a control and an nm23-H1 shRNA expression vector. Results are expressed as fold induction relative to cells without IL-6 treatment after normalization to the *GAPDH* expression ($^{*}p < 0.05$ and $^{**}p < 0.01$ for the difference from the cells transfected with control shRNA without treatment; $^{\#\#}p < 0.01$ for the difference from the 0.1 ng/mL IL-6-treated cells transfected with control shRNA; $^{++}p < 0.01$ for the difference from the 1 ng/mL IL-6-treated cells transfected with control shRNA by ANOVA for multiple comparison). (E) nm23-H1-depleted A549 cells (A549$^{shnm23\text{-}H1}$), which were genetically engineered to express shRNA-resistant nm23-H1 protein, significantly suppressed STAT3 phosphorylation with or without IL-6 treatment. (F) A549 cells stably expressing control or nm23-H1 shRNA were transfected with STAT3-responsive luciferase reporter constructs. Forty-eight hours later, the luciferase activity was measured and normalized using the dual luciferase reporter system. The normalized firefly luciferase activity was markedly increased in nm23-H1-depleted cells. The bars represent the mean (±SD) calculated from three independent experiments performed in triplicate ($^{**}p < 0.01$ for the difference from the control cells).

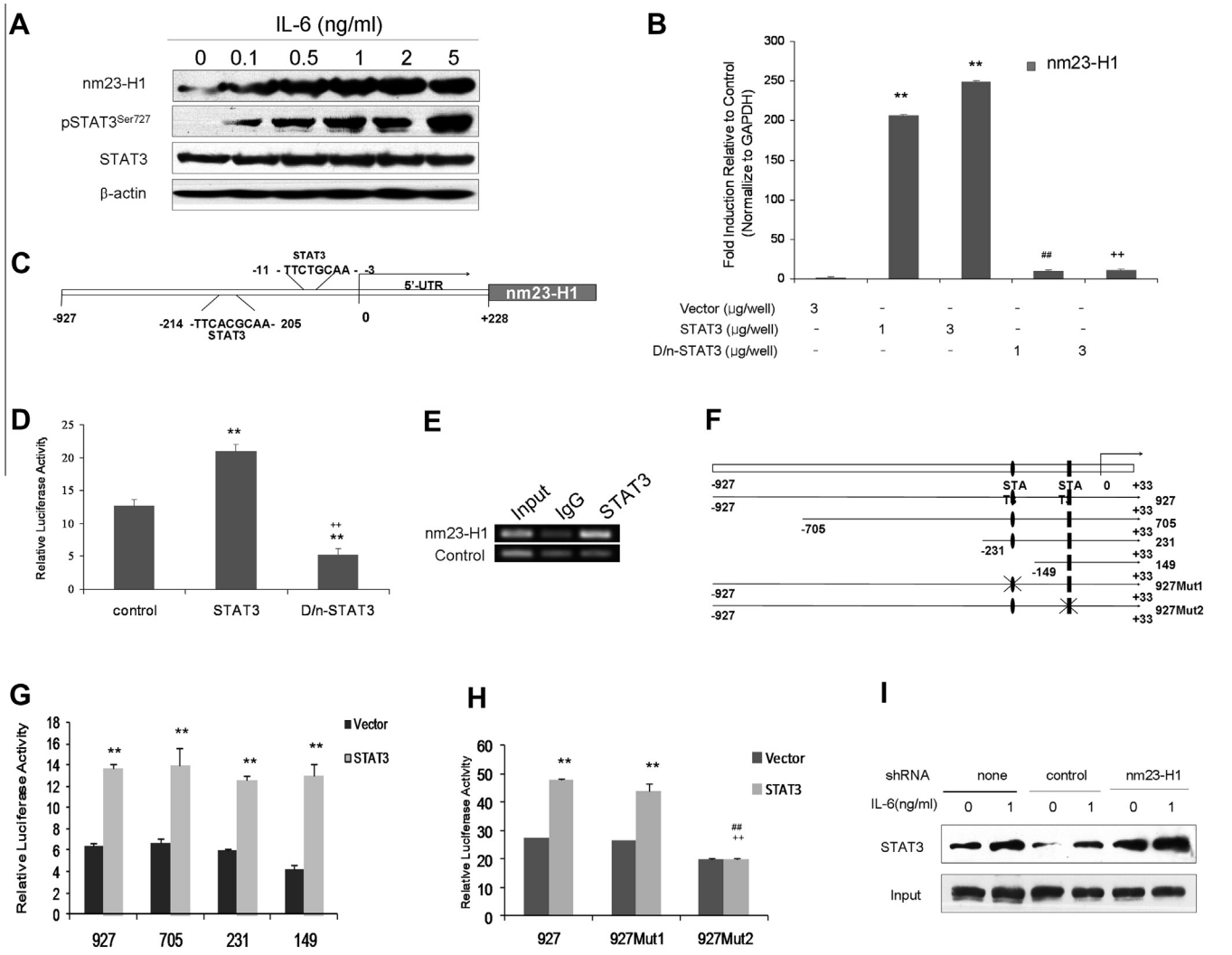

Fig. 2. Active STAT3 induces nm23-H1 expression in A549 cells. (A) Western blot demonstrated increased nm23-H1 expression following 2 h of IL-6 stimulation. (B) Forty-eight hours after transfection with an empty plasmid or a plasmid containing an expression construct for STAT3 or dominant-negative STAT3 (D/n-STAT3), total RNA was isolated, and quantitative real-time PCR was performed using the primers for nm23-H1 and *GAPDH* mRNA. The levels of nm23-H1 mRNA were markedly increased in cells overexpressing wild-type STAT3, while cells overexpressing D/n-STA3 had negligible levels of nm23-H1 mRNA ($^{**}p < 0.01$ for difference from empty plasmid transfected control cells, $^{\#\#}p < 0.01$ for the difference from the cells transfected with 1 μg STAT3 construct; $^{++}p < 0.01$ for the difference from cells transfected with 3 μg STAT3 construct by ANOVA for multiple comparison). (C) A schematic representation of the nm23-H1 promoter region showing two potential STAT3 binding sites. 5′-UTR, 5′-untranslated region. (D) A549 cells were transfected with a plasmid containing an expression construct for STAT3 or dominant-negative STAT3 and plasmids containing nm23-H1 promoter-driven luciferase or control luciferase reporter constructs. Forty-eight hours after transfection, luciferase activity was measured and normalized using the dual luciferase reporter system ($^{**}p < 0.01$ for difference from empty plasmid transfected control cells, $^{++}p < 0.01$ for the difference from cells transfected with STAT3 construct by ANOVA for multiple comparison). (E) A549 cells were subjected to ChIP assays after transfection with wild-type STAT3-expressing constructs using anti-STAT3 antibodies or control IgG. PCR using primers specific for nm23-H1 promoter showed the predicted 176-bp band for each sample. (F) Schematic representation of nm23-H1 promoter deletion constructs. (G) Forty-eight hours after transfection with one of four nm23-H1 promoter deletion constructs in Fig. 2(F) and a STAT3-expressing construct or empty vector construct as control, luciferase activity was measured and normalized. Cells transfected with constructs containing either two STAT3 binding sites (constructs 927, 705, 231) or one binding site (construct 149) showed essentially similar luciferase activity ($^{**}p < 0.01$ for difference from empty plasmid transfected control cells by ANOVA for multiple comparison). (H) A549 cells were transfected with one of three designated constructs (construct 927, 927Mut1 containing mutated STAT3 binding site 1, 927Mut2 with mutated STAT3 binding site 2) and a wild-type STAT3-expressing plasmid or an empty vector plasmid. Forty-eight hours later, luciferase activity was measured and normalized. Cells transfected with construct 927Mut2 but not 927Mut1 showed significantly decreased luciferase activity ($^{**}p < 0.01$ for difference from empty plasmid transfected control cells; $^{\#\#}p < 0.01$ for the difference from the cells transfected with construct 927; $^{++}p < 0.01$ for the difference from cells transfected with construct 927Mut1 by ANOVA for multiple comparison). (I) A549 cells stably transfected with a control or nm23-H1-specific shRNA were either left untreated or treated with IL-6 (1 ng/mL) for 1 h, and STAT3 binding to an oligonucleotide containing the STAT3 binding site 2 in the nm23-H1 promoter was detected using avidin–biotin complex DNA assays.

overnight at 4 °C on a rotator. Beads were collected by centrifugation and washed repeatedly with immunoprecipitation buffer. The precipitated beads were then boiled in Laemmli sample buffer, and STAT3 was detected by Western blot. The following STAT3 3′ biotinylated oligonucleotides were used: 5′-GTGGGCGAGCGGT GTTCTGCAAAATGGGCTCTCCGG-3′ (sense) and 5′-CCGGAGAGCC-CATTTTGCA GAACACCGCTCGCCCAC-3′ (antisense).

2.10. Statistical analysis

Data were analyzed by using the SPSS 13.0 statistical software (SPSS Inc., Chicago, IL) and are presented as means ± SD (standard deviation). Analysis of variance (ANOVA) was used to analyze the differences among different groups, and $p < 0.05$ was considered statistically significant.

3. Results and discussion

3.1. nm23-H1 negatively regulated STAT3 activity

Previous study in a mouse model showed that the level of STAT3 activity in human melanoma metastatic to brain was higher than in primary melanoma tissues [4]. We speculated that nm23-H1, which was the first metastasis-suppressor gene to be identified on the basis of an inverse relationship between nm23-H1 expression and metastasis stage, might play a role in regulating STAT3 activity. To investigate this possibility, we used an established *in vitro* model of IL-6-induced STAT3 activation and short interfering RNA (siRNA) targeting nm23-H1 to knock down its expression. The suppression of nm23-H1 expression was confirmed by both western blot (Fig. 1A) and quantitative RT-PCR (Fig. 1B). At 48 h after transfection, exposure of exogenous IL-6 in scrambled siRNA-transfected A549 cells induced tyrosine 705 phosphorylation in a dose-dependent manner, and IL-6-induced $STAT3^{Tyr705}$ phosphorylation was significantly enhanced in A549 cells transfected with siRNA specific for nm23-H1 (Fig. 1C). However, serine 727 phosphorylation of STAT3 was not appreciably affected by either exposure to IL-6 or nm23-H1 depletion. The striking difference in IL-6-induced p-$STAT3^{Tyr705}$ levels induced by nm23-H1 knockdown was mirrored by changes in its downstream target *c-Myc* (Fig. 1A and C), suggesting that IL-6-dependent induction of tyrosine phosphorylation and activity of STAT3 were inhibited by nm23-H1. To control RNAi-dependent off-target effects, we stably transfected A549 cells with a lentivirus-driven short hairpin RNA (shRNA) construct. Western blot analysis showed negligible levels of nm23-H1 protein in the nm23-H1-specific shRNA transfected cells ($A549^{shnm23\text{-}H}$) compared with control shRNA counterparts (Fig. 1C and D). Again, the levels of p-$STAT3^{Tyr705}$ were dramatically induced by IL-6 in cells transfected with control shRNA and, to a great extent, in cells with nm23-H1 shRNA. We next rescued nm23-H1 expression by transfection of shRNA-resistant nm23-H1 expression vector generated by site-directed mutagenesis of nm23-H1 cDNA into $A549^{shnm23\text{-}H}$ cells (Fig. 1E). We found that the effect of nm23-H1 depletion on IL-6-induced $STAT3^{Tyr705}$ phosphorylation was reversed by ectopic expression of shRNA-resistant nm23-H1 protein. To determine whether STAT3 transcriptional activity was also potentiated by nm23-H1 depletion, we used the luciferase reporter assay to measure STAT3-dependent transcriptional activity in nm23-H1-depleted cells (Fig. 1F). A549 cells transfected with STAT3 reporter plasmid containing seven copies of STAT3-specific binding sites from the human *C-reactive protein* (CRP) gene had a four to fivefold increase in luciferase activity compared with shScrambled control cells. Together, these findings showed that nm23-H1 negatively regulated STAT3 phosphorylation and activity of STAT3.

3.2. Active STAT3 induced nm23-H1 expression in A549 cells

The aforementioned real-time PCR indicated that IL-6 induced endogenous nm23-H1 expression in A549 cells, which was confirmed by western blot (Fig. 2A). To determine whether STAT3 mediated IL-6-induced nm23-H1 expression, we performed transfections to generate cells with increased levels of STAT3 or dominant-negative STAT3 (Fig. 2B). Overexpression of wild-type STAT3 stimulated nm23-H1 mRNA production in A549 cells, and this production was significantly lower in cells expressing dominant-negative STAT3. Examination of sequence of region upstream to the translation start site in the human nm23-H1 gene showed two putative STAT3 binding sites, −214 to −205 (site 1) and −11 to −3 (site 2) (Fig. 2C). We cloned the promoter region (from −927 to + 33) of the nm23-H1 gene into a luciferase-based reporter plasmid and co-transfected either wild-type STAT3 cDNA or dominant-negative STAT3 construct with the nm23-H1 reporter construct into A549 cells. As shown in Fig. 2D, the STAT3-stimulated nm23-H1 promoter activity was significantly inhibited by overexpression of dominant-negative STAT3. To determine whether STAT3 directly binds to the nm23-H1 promoter, ChIP assays were performed in A549 cells co-transfected STAT3 with the nm23-H1 promoter construct (Fig. 2E). PCR primers that specifically amplify a 176-bp fragment of the nm23-H1 promoter containing putative STAT3 binding sites showed a striking increase in nm23-H1 promoter immunoprecipitated by anti-STAT3 compared with control IgG. To further explore the role of STAT3 binding site in the regulation of nm23-H1 expression, we co-transfected a set of nm23-H1 reporter deletion constructs with wild-type STAT3 (Fig. 2F and G). Constructs that contained both predicted STAT3 binding sites (927, 705 and 231) or one binding site (149, site 2) still showed a significant induction of nm23-H1 promoter activity. Mutation of putative STAT3 binding site 2 prevented the induction by STAT3, whereas mutation of binding site 1 did not. Thus, STAT3 induced nm23-H1 transcription and required binding site 2, but not site 1 (Fig. 2H).

The evidence so far has led to a working model in which STAT3 activity is fine-tuned by nm23-H1 via a negative feedback mechanism; therefore, reduction or loss of nm23-H1 would lead to higher STAT3 activity. To test this hypothesis, we used biotinylated doubled-stranded oligonucleotides containing binding site 2 to immunoprecipitate active STAT3 in nm23-H1-depleted cells (Fig. 2I). Immunoprecipitation of cell homogenates with double-stranded oligos followed by western blot with an anti-STAT3 antibody showed that IL-6 treatment led to increased recruitment of STAT3 to the nm23-H1 promoter in the cells transfected with control shRNA. However, the binding of STAT3 to nm23-H1 promoter was significantly increased in nm23-H1-depleted cells.

We have identified a new function for nm23-H1 as a metastasis suppressor, acting through a negatively regulating STAT3. Aberrant STAT3 signaling has recently emerged as one of the major mechanisms for cancer progression and metastasis [13]. Constitutively active STAT3 has been found in a variety of tumors, including breast, prostate, ovarian, and lung cancers [14–17]. What's more, Huang and colleagues using a human melanoma brain metastasis animal model-found higher levels of STAT3 activity in metastatic tissues than in primary tumors [18]. In general, the amplitude of STAT3 signaling is fine-tuned via negative feedback mechanisms. The suppressor of cytokine signaling (SOCS) proteins that are activated by STAT3 have been shown to be key negative regulators of STAT3 activation [19]. Recent studies have also indicated that caveolin-1 plays a critical role in STAT3-driven invasion and metastasis of breast cancer cells [18,20].

We have demonstrated in this study that STAT3 directly binds to the nm23-H1 promoter and activates nm23-H1 expression, which in turn attenuates STAT3 activity. This feedback mechanism might provide insight into an in-built metastasis-suppressor function in tumor cells and ensure that oncogenic mutations can also activate a metastasis-suppression program to prevent tumor progression. This feedback network could be a logical new target for the design of the therapeutic strategies for treatment of early metastatic diseases. It is thus of great interest to better understand the mechanisms underlying negative regulation of STAT3 by nm23-H1.

Acknowledgments

We would like to thank Dr. Seyed Javad Moghaddam (Department of Pulmonary Medicine, The University of Texas MD Anderson Cancer Center, Houston, Texas, USA) and the Department of Scientific Publications (The University of Texas MD Anderson

Cancer Center, Houston, Texas, USA) for critical review of the manuscript and their contributions to the language editing.

References

[1] S.P. Gao, K.G. Mark, K. Leslie, W. Pao, N. Motoi, W.L. Gerald, W.D. Travis, W. Bornmann, D. Veach, B. Clarkson, J.F. Bromberg, Mutations in the EGFR kinase domain mediate STAT3 activation via IL-6 production in human lung adenocarcinomas, J. Clin. Invest. 117 (2007) 3846–3856.
[2] T. Cortas, R. Eisenberg, P. Fu, J. Kern, L. Patrick, A. Dowlati, Activation state EGFR and STAT-3 as prognostic markers in resected non-small cell lung cancer, Lung Cancer 55 (2007) 349–355.
[3] L. Song, B. Rawal, J.A. Nemeth, E.B. Haura, JAK1 activates STAT3 activity in non-small-cell lung cancer cells and IL-6 neutralizing antibodies can suppress JAK1-STAT3 signaling, Mol. Cancer Ther. 10 (2011) 481–494.
[4] T.X. Xie, F.J. Huang, K.D. Aldape, S.H. Kang, M. Liu, J.E. Gershenwald, K. Xie, R. Sawaya, S. Huang, Activation of stat3 in human melanoma promotes brain metastasis, Cancer Res. 66 (2006) 3188–3196.
[5] J. Abdulghani, L. Gu, A. Dagvadorj, J. Lutz, B. Leiby, G. Bonuccelli, M.P. Lisanti, T. Zellweger, K. Alanen, T. Mirtti, T. Visakorpi, L. Bubendorf, M.T. Nevalainen, Stat3 promotes metastatic progression of prostate cancer, Am. J. Pathol. 172 (2008) 1717–1728.
[6] P.S. Steeg, G. Bevilacqua, R. Pozzatti, L.A. Liotta, M.E. Sobel, Altered expression of NM23, a gene associated with low tumor metastatic potential, during adenovirus 2 Ela inhibition of experimental metastasis, Cancer Res. 48 (1988) 6550–6554.
[7] M.T. Hartsough, P.S. Steeg, Nm23/nucleoside diphosphate kinase in human cancers, J. Bioenerg. Biomembr. 32 (2000) 301–308.
[8] H. Miyazaki, M. Fukuda, Y. Ishijima, Y. Takagi, T. Iimura, A. Negishi, R. Hirayama, N. Ishikawa, T. Amagasa, N. Kimura, Overexpression of nm23-H2/NDP kinase B in a human oral squamous cell carcinoma cell line results in reduced metastasis, differentiated phenotype in the metastatic site, and growth factor-independent proliferative activity in culture, Clin. Cancer Res. 5 (1999) 4301–4307.
[9] Y. Fan, Y. Yao, L. Li, Z. Wu, F. Xu, M. Hou, H. Wu, Y. Shen, H. Wan, Q. Zhou, nm23-H1 gene driven by hTERT promoter induces inhibition of invasive phenotype and metastasis of lung cancer xenograft in mice, Thorac. Cancer., http://dx.doi.org/10.1111/j.1759-7714.2012.00140.x. [Epub ahead of print]
[10] M. Boissan, D. Wendum, S. Arnaud-Dabernat, A. Munier, M. Debray, I. Lascu, J.Y. Daniel, M.L. Lacombe, Increased lung metastasis in transgenic NM23-Null/SV40 mice with hepatocellular carcinoma, J. Natl. Cancer Inst. 97 (2005) 836–845.
[11] M. Luo, D. Zhu, L. Gong, X. Qiu, L. Zu, L. Sun, Z. Wu, Q. Zhou, Lentivirus-mediated stable silencing of nm23-H1 gene in lung cancer cells and the influence on biological behavior, Zhongguo Fei Ai Za Zhi 15 (2012) 139–145.
[12] Z. Wu, T.W. Lauer, A. Sick, S.F. Hackett, P.A. Campochiaro, Oxidative stress modulates complement factor H expression in retinal pigmented epithelial cells by acetylation of FOXO3, J. Biol. Chem. 282 (2007) 22414–22425.
[13] B. Tu, L. Du, Q.M. Fan, Z. Tang, T.T. Tang, STAT3 activation by IL-6 from mesenchymal stem cells promotes the proliferation and metastasis of osteosarcoma, Cancer Lett. 325 (2012) 80–88.
[14] M. Tkach, L. Coria, C. Rosemblit, M.A. Rivas, C.J. Proietti, M.C. Diaz Flaque, W. Beguelin, I. Frahm, E.H. Charreau, J. Cassataro, P.V. Elizalde, R. Schillaci, Targeting Stat3 induces senescence in tumor cells and elicits prophylactic and therapeutic immune responses against breast cancer growth mediated by NK cells and CD4+ T cells, J. Immunol. 189 (2012) 1162–1172.
[15] D. Ge, A.C. Gao, Q. Zhang, S. Liu, Y. Xue, Z. You, LNCaP prostate cancer cells with autocrine interleukin-6 expression are resistant to IL-6-induced neuroendocrine differentiation due to increased expression of suppressors of cytokine signaling, Prostate 72 (2012) 1306–1316.
[16] P. Yue, X. Zhang, D. Paladino, B. Sengupta, S. Ahmad, R.W. Holloway, S.B. Ingersoll, J. Turkson, Hyperactive EGF receptor, Jaks and Stat3 signaling promote enhanced colony-forming ability, motility and migration of cisplatin-resistant ovarian cancer cells, Oncogene 31 (2012) 2309–2322.
[17] W.P. Su, Y.C. Lo, J.J. Yan, I.C. Liao, P.J. Tsai, H.C. Wang, H.H. Yeh, C.C. Lin, H.H. Chen, W.W. Lai, W.C. Su, Mitochondrial uncoupling protein 2 regulates the effects of paclitaxel on Stat3 activation and cellular survival in lung cancer cells, Carcinogenesis 33 (2012) 2065–2075.
[18] F.J. Huang, P.S. Steeg, J.E. Price, W.T. Chiu, P.C. Chou, K. Xie, R. Sawaya, S. Huang, Molecular basis for the critical role of suppressor of cytokine signaling-1 in melanoma brain metastasis, Cancer Res. 68 (2008) 9634–9642.
[19] P.A. Johnston, J.R. Grandis, STAT3 signaling: anticancer strategies and challenges, Mol. Interv. 11 (2011) 18–26.
[20] W.T. Chiu, H.T. Lee, F.J. Huang, K.D. Aldape, J. Yao, P.S. Steeg, C.Y. Chou, Z. Lu, K. Xie, S. Huang, Caveolin-1 upregulation mediates suppression of primary breast tumor growth and brain metastases by stat3 inhibition, Cancer Res. 71 (2011) 4932–4943.